Probing the intrinsic state of a one-dimensional quantum well with photon-assisted tunneling

S. E. Shafranjuk*
Department of Physics and Astronomy, Northwestern University, Evanston, Illinois 60208, USA
(Received 2 April 2008; revised manuscript received 14 October 2008; published 12 December 2008)

The photon-assisted tunneling (PAT) through a single wall carbon nanotube quantum well (QW) is suggested for probing the Tomonaga-Luttinger liquid (TLL) state. The elementary TLL excitations inside the quantum well are density ($\rho_{\pm}$) and spin ($\sigma_{\pm}$) bosons. The bosons populate the quantized energy levels $\varepsilon_n^{\rho+}=\Delta n/g$ and $\varepsilon_n^{\rho-(\sigma\pm)}=\Delta n$ where $\Delta=hv_F/L$ is the interlevel spacing, n is an integer number, L is the tube length, and g is the TLL parameter. Since the external electromagnetic field acts on the ρ_+ bosons only whereas the neutral ρ_- and $\sigma_{\pm}$ bosons remain unaffected, the PAT spectroscopy is able of identifying the ρ_+ levels in the QW setup. The spin $\varepsilon_n^{\sigma+}$ boson levels in the same QW are recognized from Zeeman splitting when applying a dc magnetic field $H\neq 0$. Basic TLL parameters are readily extracted from the differential conductivity curves.

DOI: 10.1103/PhysRevB.78.235115 PACS number(s): 73.23.Hk, 73.40.Gk, 73.63.Hs, 78.67.De

I. INTRODUCTION

One-dimensional quantum wells (QW) give many promises for scientific research and various practical applications.[1–6] One spectacular example is the junction formed by a single wall carbon nanotube $\mathcal{T}$ with emitter $\mathcal{E}$ and collector $\mathcal{C}$ electrodes attached to its ends (see the sketch in Fig. 1). Depending on the tube properties, that setup (see Fig. 1) corresponds to various condensed-matter systems. Remarkable properties[1–10] of the carbon tubes emerge from their intrinsic structure.[1] The single wall carbon $[n,m]$ tube is a rolled up atomic honeycomb monolayer formed by two sublattices A and B. The integer indices n and m ($n\geq m\geq 0$) of the rollup vector $\mathbf{R}=n\mathbf{R}_1+m\mathbf{R}_2$ actually determine the electronic band structure of the tube. In particular, if $n-m=3k$ (k being an integer) the tube is metallic while it is semiconducting or insulating otherwise.[11] The charge carriers in metallic tubes conform to the linear dispersion law $\varepsilon_k=\pm v_F|\mathbf{k}|$ [where "±" corresponds to electrons (holes), and v_F is the Fermi velocity]. A lot of discussions address the intrinsic state of metallic tubes where the Tomonaga-Luttinger liquid state (TLL) may presumably occur.[12–16] In contrast to semiconducting tubes, where a general consensus is achieved,[1] unconventional features of the metallic tubes are not well understood yet. A lot of attention[12–16] is paid to the strong correlation effects, and to the one-dimensional transport of the electric charge carriers. Along with the TLL state in metallic tubes[12–16] under the current elaboration there are models operating with noninteracting electrons while other models exploit coupling of the tube to the external environment.[17] Although there are indications of the TLL state in the shot noise[16] and in angle-integrated photoemission measurements,[15] present experimental evidences are still indirect.[17,18] Therefore more efforts to clearly identify the intrinsic state of the one-dimensional quantum wells formed of metallic carbon tubes are required. Typical quantum well setup[6] is sketched in Fig. 1 where the one-dimensional (1D) section is denoted as $\mathcal{T}$. The bias voltage $V_{e,c}$ drops between the emitter ($\mathcal{E}$) and collector ($\mathcal{C}$) electrodes, while the gate voltage V_G is applied to the $n++$Si substrate as shown in Fig. 1. The electrochemical potentials in $\mathcal{E}$, $\mathcal{T}$, and $\mathcal{C}$ are denoted as $\mu_{e,T,c}$. The $\mathcal{E}$ and $\mathcal{C}$ electrodes are separated from the metallic tube section $\mathcal{T}$ by the interface barriers I shown in black in Figs. 1(a) and 1(b). The potential barriers emerge from differences between the Fermi velocities in the adjacent electrodes.

In this paper we suggest a method which identifies the quantized levels of charge and spin excitations in the Tomonaga-Luttinger liquid state inside the 1D quantum well shown in Figs. 1(a)–1(c). Our method exploits the fact that the electromagnetic field (EF) interacts with the charge excitations only, while the neutral particles remain unaffected. When a tunneling electron with an energy ε absorbs n photons of the external electromagnetic field, the intrinsic struc-

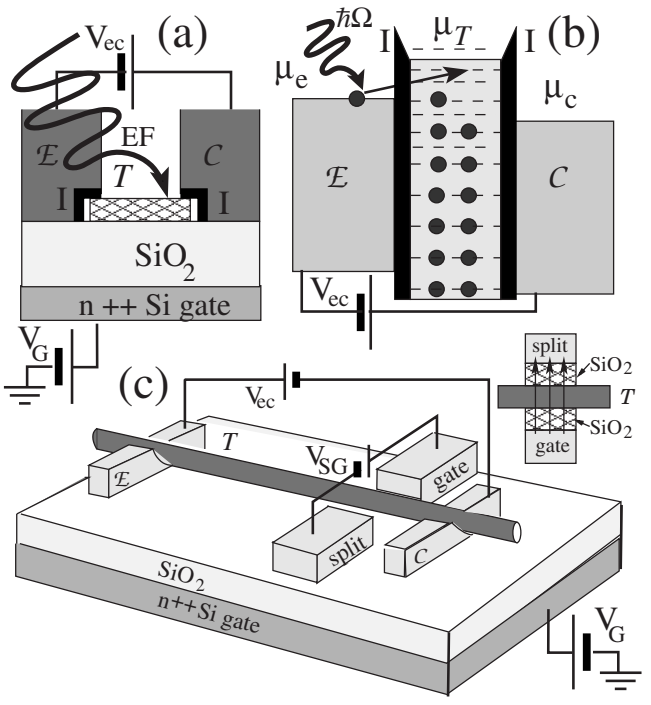

FIG. 1. (a) A quantum well composed of the 1D section $\mathcal{T}$ with attached emitter ($\mathcal{E}$) and collector ($\mathcal{C}$) electrodes. The potential barriers are shown in black at the $\mathcal{E}/\mathcal{T}$ and $\mathcal{T}/\mathcal{C}$ interfaces. (b) Energy diagram of the PAT process in the QW. (c) The split gate configuration of the QW. The right side inset shows how the electric field is applied to the $\mathcal{T}$ section.

ture of the TLL state in $\mathcal{T}$ is pronounced in the multiphoton tunneling process probability. The photon-assisted tunneling (PAT) influences probability of the single-electron tunneling (SET) which helps to elucidate the intrinsic state of the tube. In this paper we address quantum wells with long and short $\mathcal{T}$ sections. When the tube is long, the interlevel spacing $\Delta = hv_F/L$ (v_F is the Fermi velocity and L is the tube length) is small. Therefore quantization of the electron motion inside $\mathcal{T}$ is negligible. In that case the local single-electron density of states $\mathcal{N}(\varepsilon)$ inside $\mathcal{T}$ has a dip at zero energy $\varepsilon=0$. We will see that such a dip is clearly visible in the photon-assisted and in the single-electron tunneling characteristics which helps to identify the TLL state. In the opposite limit when the tube is short, the ballistic motion of the charged and neutral excitations inside $\mathcal{T}$ is quantized. During the tunneling, an electron splits into four $\rho_{\pm}, \sigma_{\pm}$ bosons (two density and two spin). The bosons populate quantized levels with different energies $\varepsilon_{\rho+} \neq \varepsilon_{\rho-(\sigma\pm)}$. The charge boson energy levels are detected with the photon-assisted tunneling.[4] We will see that the tunneling mechanism is sensitive to the emitter-collector $V_{e,c}$ and the gate V_G voltages. Therefore the TLL properties are pronounced in the differential conductivity curves of the one-dimensional quantum wells. In the same setup, the spin boson levels are fingered from Zeeman splitting $\propto \mu_B H$ when applying a finite dc magnetic field $H \neq 0$. The quantization of both the charge and spin excitations is proclaimed in the differential conductivity curves of the quantum well.

II. PHOTON-ASSISTED TUNNELING INTO THE TLL STATE

Here we address low-transparent double barrier single-wall carbon nanotube (SWCNT) junctions, assuming that the tunneling events across the $\mathcal{E}/T$ and $\mathcal{T}/\mathcal{C}$ barriers are not phase-correlated with each other. When the external ac electric-field vector directed along the tube axis, it induces an ac bias voltage $V^{(1)} \cos \Omega t$ with the field frequency Ω across the whole double-barrier junction. The ac bias voltage effectively drops on the interface barriers I, which partial resistance is assumed to be much higher than the resistance of $\mathcal{T}$. Since typical length of the carbon tube junction[5,6] is $L \sim 200$ nm–0.5 μm, the ac field wavelength of interest is 1 mm $\geq \lambda_{EF} \geq 0.5$ μm. This corresponds to the terahertz domain diapason. We describe the tunneling between the TLL state in $\mathcal{T}$ and the free-electron states in $\mathcal{E}$ ($\mathcal{C}$) electrode using the microscopic methods.[19–21] For the sake of simplicity we do not consider here the ratchet effect,[22,23] which comes either from an asymmetric scattering potential[22] or from a nonlinearity of the electronic dispersion.[23] Using methods of Refs. 19–21 one finds (see derivation details in the Appendix) the time-averaged electric current through the quantum dot in the form

$$I = \Gamma_n \frac{2e}{h} \int d\varepsilon \sum_{nm} \zeta_n \, \mathrm{Im}\, \mathcal{K}(\varepsilon) \{ J_m^2(\alpha_e)[f_+^e + \mathcal{G}_\varepsilon(f_-^e - f_+^e)] - J_m^2(\alpha_c)[f_+^c + (f_-^c - f_+^c)\mathcal{G}_\varepsilon] \}, \quad (1)$$

where $\mathcal{K}$ is the full electron correlator, $f_{\pm}^{e(c)}$ are the electron distribution functions in the $\mathcal{E}$ ($\mathcal{C}$) electrodes for which we used short notations $f(\varepsilon_{e(c)}^{m\pm}) \to f_{\pm}^{e(c)}$,

$$\varepsilon_{e(c)}^{m+} = \varepsilon + E + \hbar m\Omega + \Delta U_n^{e,c},$$

$$\varepsilon_{e(c)}^{m-} = \varepsilon + E + \hbar m\Omega + \Delta U_{n-1}^{e,c}. \quad (2)$$

In Eqs. (1) and (2) E is the energy of the occupied level in the well relative to the conductance band edge in the emitter at the zeroth dc bias voltage $V_{e,c}=0$. In Eq. (1) $\Gamma^{c(e)} = h(4\pi e^2 \nu_{e(c)} R_{e(c)})^{-1}$, $\nu_{e(c)}$ is the electron density of states inside the $\mathcal{E}(\mathcal{C})$, $R_{e(c)}$ is the tunnel resistance between the $\mathcal{E}$ ($\mathcal{C}$) electrodes and the $\mathcal{T}$ section, $\Gamma_n = \Gamma^e\Gamma^c/(\Gamma^e+\Gamma^c)$, ζ_n is the probability to find n electrons inside the well determined by a master equation (see the Appendix), and the integration is performed over the electron energy ε in the well. The Bessel function $J_m(\alpha_{e,c})$ of order m [m is the number of emitted (absorbed) photons] in Eq. (1) depends on the ac bias parameter $\alpha_{e,c} = eV_{e,c}^{(1)}/\hbar\Omega$ where $eV_{e,c}^{(1)}$ is the ac bias amplitude on the $\mathcal{E}(\mathcal{C})$ barriers, and ε is the electron energy in $\mathcal{T}$. The corresponding changes in emitter and collector electrostatic energy $\Delta U_n^{e,c}$ depend on the number n of electrons in the well as

$$\Delta U_n^e = \delta\left(n + \frac{1}{2}\right) - \eta e V_{e,c},$$

$$\Delta U_n^c = \delta\left(n + \frac{1}{2}\right) + (1-\eta) e V_{e,c}. \quad (3)$$

where $\delta = e^2/C$, $C = C_e + C_c$ is the net capacitance, $C_{e(c)}$ is the emitter (collector) capacitance, η is the fraction of the net dc bias voltage $V_{e,c}$, so that $\eta V_{e,c}$ drops between the emitter and CNT. The electron distribution function $\mathcal{G}_\varepsilon$ inside the tube entering Eq. (1) must in general be obtained from a corresponding quantum kinetic equation.[20] However for the sake of simplicity we will follow a procedure suggested in Ref. 24. Namely, we approximate $\mathcal{G}_\varepsilon$ by a Fermi-Dirac distribution, but with a finite chemical potential $\mu_{\mathcal{T}} \neq 0$ in the form

$$\mathcal{G}_\varepsilon \to \mathcal{G}_0(\varepsilon) = \frac{1}{\exp[(\varepsilon - \mu_{\mathcal{T}})/T] + 1}. \quad (4)$$

A similar quasiequilibrium approximation had formerly also been used for describing of nonequilibrium superconductors.[25] The chemical potential $\mu_{\mathcal{T}}$ of electrons in $\mathcal{T}$ entering Eq. (4) is defined by the expression for the mean number of electrons

$$\langle n \rangle = \frac{2}{h}\frac{1}{\Gamma^e + \Gamma^c} \int d\varepsilon \sum_{nm} \zeta_n \, \mathrm{Im}\, \mathcal{K}(\varepsilon) \{ \Gamma^e J_m^2(\alpha_e) \times [1 - 2f_-^e + 2(f_-^e - f_+^e)\mathcal{G}_\varepsilon] + \Gamma^c J_m^2(\alpha_c)[1 - 2f_-^c + 2(f_-^c - f_+^c)\mathcal{G}_\varepsilon] \} + \langle n_G \rangle, \quad (5)$$

where $\langle n_G \rangle$ is the number of extra electrons induced by the gate voltage $V_G \neq 0$ applied as shown in Fig. 1. When the ac bias is off ($\alpha_{e,c} \to 0$), Eq. (1) yields a well-known formula for the electric conductivity of a double-barrier low transparent tunneling junction.[24] In equilibrium and in absence of SET one sets $\mu_{\mathcal{T}} \equiv 0$ and the distribution function $\mathcal{G}_0(\varepsilon)$ in Eq. (1) disappears. In the last case one also uses $f_{\pm}^{e(c)}(\varepsilon) = f_0(\varepsilon)$

$=1/(\exp[\varepsilon/T]+1)$, where T is the temperature. Then one simply gets

$$\sigma = (2e^2/h)\Gamma_n \bar{M}(eV_{e,c}), \tag{6}$$

where $\bar{M}(eV_{e,c})=\int_{-\infty}^{\infty} d\varepsilon \mathcal{N}(\varepsilon)[-\partial f_0(\varepsilon - eV_{e,c})/(\partial\varepsilon)]$ and $\mathcal{N}(\varepsilon)$ is the single-electron density of states. The comb-shaped free-electron density of states in the well is

$$\mathcal{N}(\epsilon) = \frac{1}{\pi}\mathrm{Im}\sum_m \frac{1}{\epsilon - \Delta m - i\gamma_n}, \tag{7}$$

where Δ is the level spacing, γ_n is the quantized level width (in the case of interest $\gamma_n \ll \Delta$), and h is the Plank constant.

III. TLL TUNNELING DENSITY OF STATES OF A LONG QW

If the metallic tube section $\mathcal{T}$ is long, $L > v_F\tau_T$ (where $\tau_T=\hbar/\Gamma_n$ is the net tunneling time), the quantization inside $\mathcal{T}$ is negligible. The level separation for typical carbon tube junctions[5,6] becomes indistinguishable when $L \geq 3$ μm. Strong electron correlations drive the electron system into the *Tomonaga-Luttinger liquid* state.[12,14,16] According to Eq. (1), the electric current is expressed via the single-electron correlator $\mathcal{K}$, which is related to the spectral density $\mathcal{A}_\kappa(\varepsilon)$ of the right-moving ($\kappa=1$) fermions as

$$\mathcal{A}_1(\varepsilon) = \mathrm{Im}\, G_1^R(q=0, \varepsilon + i\delta) = -\,\mathrm{Im}\, \mathcal{K}(\varepsilon + i\delta)/\pi. \tag{8}$$

At zero temperature $T=0$ following Ref. 19 one finds

$$\mathcal{K}(\varepsilon) = -\sqrt{2/\pi i}|\varepsilon|^{2\gamma}\sin(\pi\gamma)[2(-1)^\gamma\gamma\Gamma(-2\gamma-1)|\varepsilon| + e^{i\pi\gamma}\,\mathrm{sign}(\varepsilon)\{\Gamma(-2\gamma) + g^2(r^2/v_F^2)\gamma(2\gamma+1) \times\Gamma[-2(\gamma+1)]\varepsilon^2\}], \tag{9}$$

where $\Gamma(x)$ is the gamma function of x, r is the cutoff parameter, $\gamma=(g^{-1}+g-2)/8$, and g is the Luttinger liquid parameter. In the limit $g\to 1$, the expression for $\mathcal{A}_\kappa(\varepsilon)$ transforms to the free-electron spectral density $\mathcal{A}_\kappa^{(0)}(\varepsilon) = \mathrm{sign}\,\varepsilon/(\sqrt{2}\pi v_F)$. Properties of the TLL state are sensitive to the Luttinger parameter g. The single-electron density of states $\mathcal{N}(E)$ of a one-dimensional quantum well with a long $\mathcal{T}$ section is shown for different values of g in Figs. 2(a) and 2(b). The Luttinger parameter g can be controlled either by the gate voltage V_G or by the split gate voltage V_{SG} as shown in Fig. 1(c) [see also the right side inset there].

Since the gate voltage V_G affects the charge density q on $\mathcal{T}$, $q=CV_G$ (where the capacitance $C=2\pi\epsilon_0 L/\cosh^{-1}(2h_T/d)$, ϵ_0 is the vacuum permittivity, d is the tube diameter, and h_T is the distance from the tube to substrate) it allows changing of g. An altering of V_G renormalizes $g\to g+\beta_G V_G$ due to changes in the dielectric function $\epsilon(k,\varepsilon)$ and in the Coulomb screening. According to Refs. 12 and 26, the Luttinger parameter g for a carbon tube depends on the electrostatic energy U_n as

$$g \simeq \frac{1}{\sqrt{1+2U_n/\Delta}}, \tag{10}$$

where $\Delta=hv_F/L$ is the energy-level spacing while the change of U_n is determined by Eq. (3). A simple evaluation

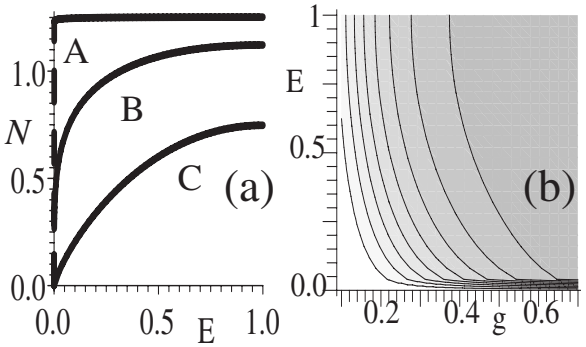

FIG. 2. (a) The single-electron density of states inside the $\mathcal{T}$ section of an QW for the Luttinger parameter $g=1$ (curve A), 0.4 (curve B), and $g=0.2$ (curve C). (b) Contour E-g plot of the single-electron density of states (DOS) inside the $\mathcal{T}$ section.

from the band-structure calculations[7] gives $\beta_G=0.005-0.03$ depending on directions of the rollup vector $\mathbf{R}$. The $\mathcal{N}(E)$ shape is also controlled with V_{SG} utilizing the split gate configuration[7] as shown in Fig. 1(c). The electric field in that setup is perpendicular to the tube axis as shown in the right inset of Fig. 1(c). The split-gate setup allows driving the tube electron state from the semiconducting to the metallic one. The transversal electric field induces a finite dipole momentum directed in perpendicular to the tube, which renormalizes g as well. The corresponding alteration of the Luttinger parameter g is evaluated using, e.g., results of Refs. 27–29. This gives $g\to gJ_0^{-1}(V_{SG}d/\hbar v_F)$. For a narrow-gap semiconducting $\mathcal{T}$ (see Ref. 7) and for typical parameters of the tube quantum well, the split gate induced change is $g\to g+\beta_{SG}V_{SG}$ where $\beta_{SG}=0.01-0.05$ for different rollup vectors. If the transversal electric field V_{SG}/d inside $\mathcal{T}$ is sufficiently strong, one induces a semiconducting-metal transition.[27–29] The electronic properties of the tube then switch from a one-dimensional narrow gap semiconductor to the TLL.[30]

The time-averaged conductance $\sigma(V_{e,c})$ of the long CNT junction exposed to an external electromagnetic field is computed using Eqs. (1)–(3), (5), (8), and (9). We calculate $\sigma(V_{e,c})$ and the electric current $I(V_{dc})$ [$V_{dc}=(V_{e,c}-V_t)\eta$ is the reduced voltage, $V_t=(E-\epsilon_F)/e\eta$ is the SET threshold voltage] for the two cases of interest. One limit corresponds to $\delta \ll T$ when the single-electron tunneling is not essential [$\delta = e^2/C$, $C=C_e+C_c$ is the net capacitance of the double-barrier junction, $C_{e(c)}$ is the emitter (collector) capacitance]. Then Eq. (1) for the tunneling current through the quantum well is reduced to

$$I(V_{e,c}) = \frac{2e}{h}\Gamma_n\sum_m \int d\varepsilon\ \mathrm{Im}\,\mathcal{K}(\varepsilon,\Omega)[J_m^2(\alpha_e)f(\varepsilon_m^e) - J_m^2(\alpha_c)f(\varepsilon_m^c)], \tag{11}$$

where now

$$\varepsilon_m^e = \varepsilon_{e,c} - \eta e V_{e,c} + \hbar m\Omega,$$

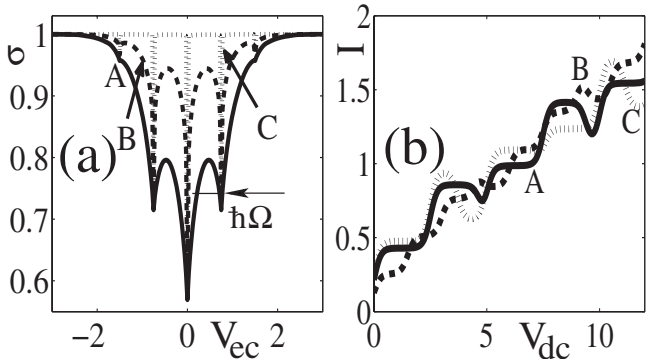

FIG. 3. (a) Splitting of the zero-bias TLL dip in the differential tunneling conductivity $\sigma(V_{e,c})$ [in units of $e^2 v_F N(0)$] in a long carbon nanotube CNT junction due to the photon-assisted tunneling. Spacing between the zero dip and adjacent satellite dips is $\hbar\Omega$. (b) The Coulomb staircase in the PASET current-voltage characteristics $I(V_{\rm dc})$ versus reduced voltage $V_{\rm dc}$ (see text) of the CNT junction in the TLL state with $g=0.4$ under influence of the ac bias field with the amplitude $eV^{(1)}=3.4$ (in units of $\delta=e^2/C$) and for a symmetric junction ($\eta=0.5$). Curve A corresponds to $\Omega=4.7$, curve B to $\Omega=3.7$, and curve C to $\Omega=6.7$.

$$\varepsilon_m^c = \varepsilon_{e,c} + (1-\eta)eV_{e,c} + \hbar m\Omega. \tag{12}$$

The above equations [Eqs. (11) and (12)] are completed by Eq. (8) to compute the dc differential tunneling conductance $\sigma(V_{e,c})$. The results are shown in Fig. 3(a) where we plot $\sigma(V_{e,c})$ of a long CNT junction in conditions of the photon-assisted tunneling for $\Omega=0.75$, $eV^{(1)}=0.65$, and for three distinct values of the Luttinger liquid parameters $g=0.2$ (curve A), $g=0.4$ (curve B), and $g=0.93$ (curve C). One may notice that the zero-bias dip in $\sigma(V_{e,c})$, which was positioned at $V_{e,c}=0$ when the ac field was off ($eV^{(1)}=0$), splits into additional satellite peaks spaced by $\hbar\Omega$.

Another limit corresponds to the single-electron tunneling which occurs if the condition

$$eV_{e,c}/2 - E - \hbar m\Omega - \delta(n+1/2) \le \mu_{\mathcal{T}}(n) \le eV_{e,c}/2 - E - \hbar m\Omega - \delta(n-1/2) \tag{13}$$

is fulfilled. The condition (13) can be independently accomplished by adjusting Ω, $V_{e,c}$, and $V_{\rm G}$ (which alters n). The zero-temperature conductivity for a symmetric junction then takes the form

$$\sigma(V_{e,c}) = \frac{\partial I(V_{e,c})}{\partial V_{e,c}} = \frac{2e}{h}\Gamma_{e,c}\sum_m J_m^2(\alpha)\zeta_n\{\mathrm{Im}\,\mathcal{K}[\mathcal{E}_+^m(n)] + \mathrm{Im}\,\mathcal{K}(\mathcal{E}_{n-}^m)\theta[\mu_{\mathcal{T}}(n) - \mathcal{E}_{n-}^m] - \mathrm{Im}\,\mathcal{K}(\mathcal{E}_{n+}^m)\theta[\mu_{\mathcal{T}}(n) - \mathcal{E}_{n+}^m]\}, \tag{14}$$

where ζ_n is the probability to find n electrons inside the well,

$$\mathcal{E}_{n\pm}^m = eV_{e,c} - E - \hbar m\Omega - \delta\left(n \pm \frac{1}{2}\right),$$

and E is the occupied level energy in the quantum well relative to the conductance band edge in the emitter in absence of the bias voltage. Equation (14) can be overwritten in the shorter form

$$\sigma(V_{e,c}) = \frac{2e}{h}\Gamma_{e,c}\sum_m J_m^2(\alpha)\zeta_n \cdot \mathcal{A}(n,m), \tag{15}$$

where

$$\mathcal{A}(n,m) = \begin{cases} \mathrm{Im}\,\mathcal{K}(\mathcal{E}_{n+}^m) & \text{if } \mu_{\mathcal{T}}(n) < \mathcal{E}_{n+}^m \\ 0 & \text{if } \mathcal{E}_{n+}^m < \mu_{\mathcal{T}}(n) < \mathcal{E}_{n-}^m \\ \mathrm{Im}\,\mathcal{K}(\mathcal{E}_{n-}^m) & \text{if } \mu_{\mathcal{T}}(n) > \mathcal{E}_{n-}^m, \end{cases}$$

since one always gets $\mathcal{E}_{n+}^m < \mathcal{E}_{n-}^m$. To consistently describe the single-electron tunneling Eqs. (1)–(3) must be completed by an equation for $\mu_{\mathcal{T}}(n)$. For a symmetric junction ($\alpha_e=\alpha_c$) one gets

$$\langle n_{\rm G}\rangle + \langle n\rangle = \frac{4}{h}\sum_{n,m} J_m^2(\alpha)\zeta_n \int d\varepsilon\ \mathrm{Im}\,\mathcal{K}(\varepsilon) \times [1 - f_-^{e,c} + (f_-^{e,c} - f_+^{e,c})\mathcal{G}_\varepsilon],$$

where

$$f_\pm^{e,c} = f\left(\varepsilon + E + \hbar m\Omega + \delta\left(n \pm \frac{1}{2}\right) - eV_{e,c}/2\right) + f\left(\varepsilon + E + \hbar m\Omega + \delta\left(n \pm \frac{1}{2}\right) + eV_{e,c}/2\right)$$

and $\mathcal{G}_\varepsilon$ is approximated by Eq. (4), $n_{\rm G}$ is the additional electron density induced by a finite gate voltage $V_{\rm G}\neq 0$. The condition which determines the (k,m)th (k being the integer single-electron tunneling index, m being the integer PAT index) vertical step in the $I(V_{e,c})$ [or a sharp peak in $\sigma(V_{e,c})$] is

$$e\eta(V_{k-1,k}^m - V_t) = \delta(k-1) + \varepsilon + m\hbar\Omega,$$

where k is integer. At $\alpha_{e,c}=0$ one gets

$$V_{k-1,k} = V_t + \frac{\delta(k-1)+\varepsilon}{e\eta}.$$

The spacing between two adjacent steps at $\alpha_{e,c}=0$ is

$$V_{k,k+1} - V_{k-1,k} = \frac{\delta + \varepsilon_{k+1} - \varepsilon_k}{e\eta} \tag{16}$$

when the external ac field is finite ($\alpha_{e,c}\neq 0$); the steps split additionally by $\pm\hbar\Omega$.

The current-voltage characteristics $I(V_{\rm dc})$ [where $V_{\rm dc}=(V_{e,c}-V_t)\eta$] in condition of the photon-assisted single-electron tunneling (PASET) across the quantum well in the Tomonaga-Luttinger liquid state are shown in Fig. 3(b). According to Ref. 24, the equilibrium shape of the $I(V_{\rm dc})$ curves (quoted as Coulomb staircase) is extremely sensitive to the double-barrier junction's parameters such as barrier transparencies, capacitance, symmetry, purity of the carbon tube section, and the energy-level spacing. The photon-assisted tunneling induced by the external electromagnetic field introduces additional features in those curves. We have computed PASET curves for a QW with a long $\mathcal{T}$ section where the single-electron tunneling takes place. The external

$\hat{x}$-polarized electromagnetic field induces an ac bias voltage across the junction as $V^{(1)}\cos\Omega t$. The most remarkable elements of the $I(V_{dc})$ curves *A*-*C* in Fig. 3(b) are local dips which originate from an interference between the zero-energy TLL anomaly pronounced in equilibrium at $\varepsilon=0$ [see Fig. 2(a)] and the photon-assisted single-electron tunneling (PASET) processes. The Coulomb staircase curve *A* in Fig. 3(b) corresponds to $\Omega=4.7$, curve *B* to $\Omega=3.7$ and curve *C* to $\Omega=6.7$ computed for $g=0.4$.

IV. IDENTIFYING OF THE CHARGE AND THE SPIN BOSON ENERGY LEVELS

In a opposite limit when the $\mathcal{T}$ section is short, the quantized energy levels are well resolved since the condition $\Gamma^{e,c}\ll\Delta$ is observed ($\Gamma^{e,c}$ are the $\mathcal{E}\Leftrightarrow\mathcal{T}$ and $\mathcal{T}\Leftrightarrow\mathcal{C}$ electron tunneling rates, and $\Delta=hv_F/L$ is the interlevel spacing inside $\mathcal{T}$). In this section we neglect the single-electron tunneling contribution[24] (Coulomb blockade phenomena). That is justified when the temperature T is not too low, $T\gg\Gamma^{e,c}$. In that limit we use Eq. (11) again but with a different Im $\mathcal{K}(\varepsilon)$ which now acquires a comblike shape. Due to the spin-charge separation in the Tomonaga-Luttinger liquid there are two sets of quantized energy levels in a low-transparent quantum well with a short $\mathcal{T}$ section. For the QW transparency $\tilde{T}=0.3$ [where $\tilde{T}=4\pi\Gamma_n L_n/(\hbar v_F)$, $L_n=L_e+L_c$, where L_e and L_c are the $\mathcal{E}$ and $\mathcal{C}$ thicknesses respectively, $v_F=8.1\times10^5$ m/s] one gets $\Gamma_n\approx0.3$ meV. For the tube length $L=3$ μm one obtains spacing between the quantized levels as $\Delta=1$ meV. The photon-assisted processes cause an additional splitting ~0.6 meV which corresponds to the ac bias frequency $\Omega\approx1$ THz. Following to Refs. 12 and 21 one defines the transmission coefficient as $\tilde{T}(E)=|i\hbar G^R(L,E)|^2$. We assume that coupling of the single wall tube segment $\mathcal{T}$ to the external $\mathcal{E}$ and $\mathcal{C}$ electrodes is weak. In this approximation we compute the local electron density of states $\mathcal{N}(\varepsilon)$ implementing boundary conditions[12] for the electron wave function inside a short carbon tube section $\mathcal{T}$. Then the quantized energy levels are firmly separated from each other and resolved. The retarded single-electron Green's function is $G^R(L,t)=\Pi_a\mathcal{G}_a^R(L,t)$, in which Fourier transform has a comblike shape

$$G_n^R(L,\varepsilon)=i\sqrt{\frac{2}{\pi}}\sum_a\frac{4^{g_a^-}\sin^{2g_a^-}(\pi\lambda/L)}{\varepsilon_a},$$

$$\sum_n\Theta_n(-1)^{-2g_a^++n}\frac{\Gamma(1-2g_a^++n)\Gamma(\varepsilon/\varepsilon_a)}{\Gamma(1-2g_a^++n+\varepsilon/\varepsilon_a)},\qquad(17)$$

where $a=(\rho_\pm,\sigma_\pm)$ is the TLL boson index, i.e., $\varepsilon_n^{\rho+}=\Delta/g$ while $\varepsilon_n^{\rho-(\sigma\pm)}=\Delta$, Θ_n are the coordinate-dependent coefficients inside the tube and the length parameter $\lambda\ll L$ effectively incorporates influence of the interface barriers,[12] n is the quantization index, and $g_a^\pm=(1/g_a\pm g_a)/16$. The parameters Θ_n and λ are determined by the integer charge and by the sum of phase shifts at the interfaces. The charge ρ_+ bosons populate the energy levels $\varepsilon_n^{\rho+}=hv_Fn/Lg=n\Delta/g$ (where n is integer number), while three other neutral ρ_-- and $\sigma_\pm$-boson energy levels have conventional values $\varepsilon_n^{\rho-(\sigma\pm)}=hv_Fn/L=n\Delta$. The tunneling differential conductivity $\sigma(V_{e,c})$ of a "clean" (i.e., without impurities on $\mathcal{T}$) sample is a combination of two combs with different periods shown in Fig. 4(a) for $g=0.23$. One of the combs corresponds to the ρ_+ boson, while another comb is related to the three remaining neutral $(\rho_-,\sigma_+,\sigma_-)$ bosons. In the steady state, when the EF is off (i.e., $\alpha_{e,c}\equiv0$), during the tunneling say, from $\mathcal{E}$ to $\mathcal{T}$, an electron splits into four bosons as $e\rightarrow\rho_++\rho_-+\sigma_++\sigma_-$, which assumes the energy conservation as

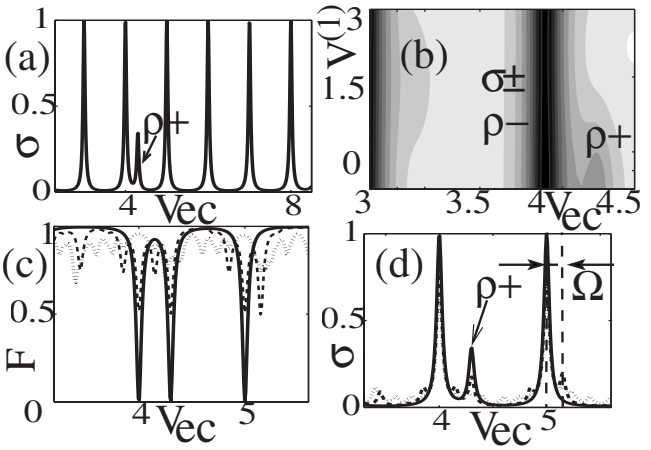

FIG. 4. (a) The steady-state tunneling differential conductivity $\sigma(V_{e,c})$ [in units of $e^2v_FN(0)$] in the TLL state. The peak at $V_{e,c}=4.3$ (in units of Δ/e) corresponds to the ρ_+ boson. (b) The contour plot $\sigma(V_{e,c},V_{e,c}^{(1)})$ [$V_{e,c}$ and the ac bias amplitude $V_{e,c}^{(1)}$ being in units of Δ/e]. (c) The Fano factor $F(E)$ of the QW in conditions of PAT. (d) $\sigma(V_{e,c})$ for different Ω.

$$E+\eta eV_{e,c}=\varepsilon_n^{\rho+}+\varepsilon_n^{\rho-}+\varepsilon_n^{\sigma+}+\varepsilon_n^{\sigma-}=n(3+1/g)\Delta\qquad(18)$$

(n being the integer number). That corresponds to a resonance tunneling through the quantized TLL states tuned by $V_{e,c}$. However, if the electromagnetic field is on ($\alpha_{e,c}\neq0$), the resonance tunneling condition changes. That happens because the ac field acts on the charge ρ_+ bosons only, which absorb the EF photons during the photon-assisted tunneling processes. The photons do not excite the neutral ρ_- and $\sigma_\pm$ bosons since they do not interact with the external electromagnetic field. The ac field-modified resonance condition depends on both $V_{e,c}$ and Ω simultaneously

$$\begin{aligned}E+\eta eV_{e,c}&=(\varepsilon_n^{\rho+}+m\hbar\Omega)+\varepsilon_n^{\rho-}+\varepsilon_n^{\sigma+}+\varepsilon_n^{\sigma-}\\&=n(3+1/g)\Delta+m\hbar\Omega,\end{aligned}\qquad(19)$$

where n and m are integer numbers. The external electromagnetic field splits the conductivity peaks selectively. Because $V_{e,c}$ and Ω are bound by the condition (19), this imposes a constrain on the net photon-assisted tunneling resonant current through the quantum well. Using Eq. (19) one immediately extracts g and Δ from the dc PAT current-voltage characteristics. More specifically, the value of g and Δ follows right from periods of the two steady-state combs $\sigma(V_{e,c})$ shown in Fig. 4(a). This is illustrated by the PAT differential tunneling conductivity $\sigma(V_{e,c})$ for $\alpha_{e,c}\neq0$ shown in Figs. 4(b) and 4(d). Figure 4(b) is the contour plot

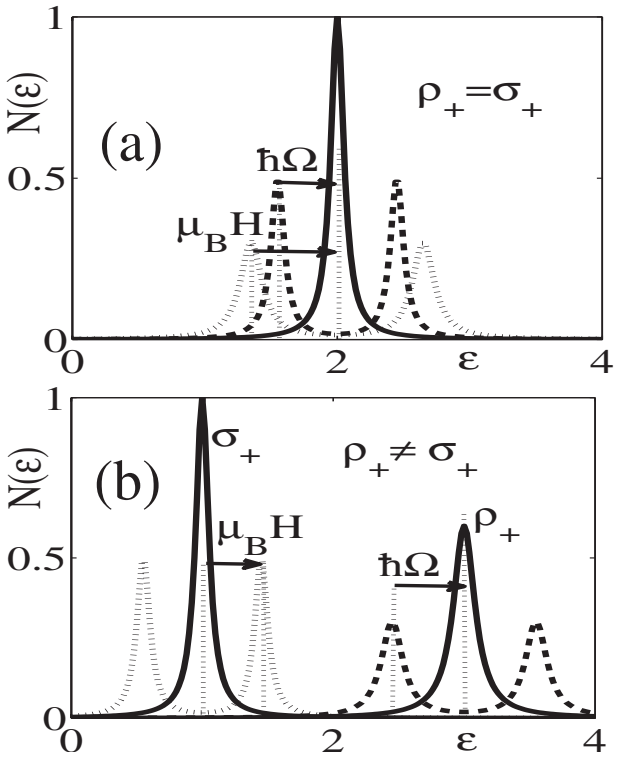

FIG. 5. Splitting of quantized levels due to the photon assisted tunneling and Zeeman effect as pronounced in the single-electron density of states $N(\varepsilon)$ of a short CNT junction. (a) A free-electron quantized level (solid curve) for which the charge ρ_+ and spin σ_+ bosons coincide splits by an ac electromagnetic field (with spacing $\propto\hbar\Omega$) and by a dc magnetic field (with spacing $\propto\mu_B H$) simultaneously. (b) The quantized levels of spin σ_+ and charge ρ_+ bosons have different energies $\varepsilon_n^{\rho+}\neq\varepsilon_n^{\sigma+}$ in the TLL state. The ac bias splits the charge boson levels (dashed curve on the right) while the dc magnetic field splits the spin boson levels (dotted curve on the left) only. The charge boson localized energy level $\varepsilon_n^{\rho+}$ splits in the two satellite peaks with spacing $2\hbar\Omega$. Although the ac field has no influence on the neutral spin bosons, the spin level $\varepsilon_n^{\sigma+}$ splits (Ref. 12) in two sublevels spaced with $\Delta_Z\propto\mu_B H$ (both in units of Δ) due to the Zeeman effect when a dc magnetic field $H\neq 0$ is applied.

$\sigma(V_{e,c},V_{e,c}^{(1)})$ ($V_{e,c}$ and the ac bias amplitude $V_{e,c}^{(1)}$ being in units of Δ/e). The same quantity $\sigma(V_{e,c})$ but for fixed $\Omega=0.85$ and $eV_{e,c}^{(1)}=0.01$ (solid curve), $eV_{e,c}^{(1)}=1$ (dashed curve), and $eV_{e,c}^{(1)}=5$ (dotted curve) is presented in Fig. 4(d). In an experiment one obtains series of peaks in the differential conductivity $\sigma(V_{e,c})=\partial I/\partial V_{e,c}$ curves for the steady state ($\alpha_{e,c}\equiv 0$). When the ac field is on ($\alpha_{e,c}\neq 0$) one also gets the satellite PAT peaks with an additional spacing $\Delta\rightarrow\Delta\pm\hbar m\Omega$ as shown in Figs. 4(c) and 4(d). Then one determines the ratio $r_1=A_1^{\rho+}/A_0^{\rho+}$ where $A_{0(1)}^{\rho+}$ is the ρ_+-boson peak height, which corresponds to the number of emitted (absorbed) photons $m=0,1$. The ratio r_1 allows extracting of the actual ac field amplitude $V^{(1)}$ acting on the junction. The splitting of the charged ρ_+ boson peaks by the ac field helps in identifying the Tomonaga-Luttinger liquid state. The method is illustrated further in Fig. 5 where we show a single peak in $\mathcal{N}(\varepsilon)$ corresponding to a quantized free-electron energy level [see Fig. 5(a)]. For noninteracting electrons ($g=1$) the same single level splits either by an ac field due to the photon-assisted tunneling phenomena with spacing $\propto m\hbar\Omega$ (m being integer) or by a dc magnetic field with the Zeeman spacing $\propto\mu_B H$. The situation is remarkably different in the Luttinger liquid state when $g\neq 1$ and the charge ρ_+ and spin σ_+ levels have distinct energies $\varepsilon_n^{\rho+}\neq\varepsilon_n^{\sigma+}$. Then one easily identifies the charge and spin levels merely by applying the ac field and dc magnetic field to the same quantum well. If a level splits with spacing $\propto m\hbar\Omega$ by the ac field only (showing no response to the dc field) then it certainly is a ρ_+ charge boson level ($g\neq 1$). If it splits by the dc magnetic field[12] with the Zeeman spacing $\propto\mu_B H$ showing no response to the ac field, then it must be associated with the spin bosons σ_+. However if both ac and dc magnetic fields split the same level, then the level belongs to the noninteractive electrons ($g=1$) as had been said above. In this way one perceives the charge and spin bosons in experiments when applying ac electromagnetic field in combination with the dc magnetic field to a carbon tube junction. An important requirement to the experimental metallic carbon tube quantum well samples is that they must be clean. An electron-impurity scattering in real samples leads to a formation of additional pairs of combs with different periods. Then, an identification of the TLL state becomes possible with a mere generalization of the method described above.

Ratio of the noise power to the mean current (Fano factor) is computed as $F=\Sigma_n T_n(1-T_n)/\Sigma_n T_n$ where the summation is performed over the conducting channels. The result is shown in Fig. 4(c). One can see that at the energies of quantized levels the noise is much lower than the Poisson noise of a conventional tunnel junction where $F=1$. Remarkably, the multiphoton absorption is pronounced in the noise spectra as well. In this way Fig. 4(c) suggests a method of the noise spectroscopy for studying of the photon-assisted tunneling into the TLL state.

V. CONCLUSIONS

Phenomena considered in this paper originate from a specific physics of the charge and spin carriers, behaving like a blend of four noninteracting bosons. The Tomonaga-Luttinger liquid state occurs inside the one-dimensional quantum well formed by a metallic single wall carbon tube. The TLL state is tested with applying of an external ac electromagnetic field and of a dc magnetic field simultaneously. The ac field splits the charge boson energy levels due to the photon-assisted tunneling while the dc magnetic field splits the spin boson levels due to the Zeeman effect. That allows a mere identification of the quantized energy levels associated with the charge and spin bosons forming the TLL state in relevant experiments. Besides, one also determines the quantized level spacing Δ and the TLL parameter g. The unconventional electronic and photonic properties of the metallic carbon tube quantum well can be utilized in various nanodevice applications including terahertz field sensors and nanoemitters.

ACKNOWLEDGMENTS

I wish to thank V. Chandrasekhar and P. Barbara for fruit-

ful discussions. This work was supported by AFOSR Grant No. FA9550–06–1-0366.

APPENDIX

Here we derive analytical expressions for the time-averaged electric current through the TLL quantum well in conditions of the photon-assisted single-electron tunneling. The external electromagnetic field is applied to the tube junction as shown in Fig. 1. Our model describes a low transparency junction which average conductance is small, $G \ll R_Q^{-1}$ where $R_Q = \pi\hbar/2e^2 \simeq 6.5$ kΩ. Since coupling to the electrodes is weak, the emitter-tube ($\mathcal{E} \Leftrightarrow \mathcal{T}$) and the tube-collector ($\mathcal{T} \Leftrightarrow \mathcal{C}$) tunneling processes are assumed as being not phase correlated. The SET dynamics in that approximation is well described by a simple master equation.[24] The external electromagnetic field with frequency Ω induces an ac bias voltage $V^{(1)}\cos\Omega t$ with amplitude $V^{(1)}$ across the junction. The ac voltage modulates phases of the tunneling electrons as $\phi^{e,c}(t) = (eV_{e,c}^{(1)}/\hbar)\int^t \cos\Omega t' dt'$ where $V_e^{(1)} = \eta V^{(1)}$, $V_c^{(1)} = (1-\eta)V^{(1)}$ are corresponding fractions of the ac voltage drop on the emitter and collector, η is the fraction of the net ac bias voltage $V^{(1)}$, so $\eta V^{(1)}$ drops between the emitter and CNT. The time-averaged single-electron tunneling electric current through the double barrier junction is expressed via partial tunneling rates $w_+^{e,c}$ and $w_-^{e,c}$ from emitter (collector) to the energy levels inside the well,[24]

$$w_+^{e,c}(n,m) = J_m^2(\alpha_{e,c}) \int d\varepsilon \Gamma_\varepsilon^{e,c}(\varepsilon_{e(c)}^{m+}) f(\varepsilon_{e(c)}^{m+}) G_m^-(\varepsilon,\Omega),$$

$$w_-^{e,c}(n,m) = -J_m^2(\alpha_{e,c}) \int d\varepsilon \Gamma_\varepsilon^{e,c}(\varepsilon_{e(c)}^{m-})[1 - f(\varepsilon_{e(c)}^{m-})] G_m^+(\varepsilon_k,\Omega),$$

$$w_{nm}^{\pm} = w_\pm^e(n,m) + w_\pm^c(n,m), \tag{A1}$$

where the integration is performed over the electron energy ε in the well, E is the energy of the occupied level in the well relative to the conductance band edge in the emitter at the zeroth dc bias voltage $V_{e(c)}=0$, m is the number of emitted (absorbed) photons, and the electron energy arguments are

$$\varepsilon_{e(c)}^{m+} = \varepsilon + E + \hbar m\Omega + \Delta U_n^{e,c},$$

$$\varepsilon_{e(c)}^{m-} = \varepsilon + E + \hbar m\Omega + \Delta U_{n-1}^{e,c}.$$

The Bessel function $J_m(\alpha_{e,c})$ of order m in Eq. (A1) depends on the ac bias parameter $\alpha_{e,c} = eV_{e,c}^{(1)}/\hbar\Omega$. Corresponding changes $\Delta U_n^{e,c}$ of the emitter and collector electrostatic energies depend on the number n of electrons in the well as

$$\Delta U_n^e = \delta\left(n + \frac{1}{2}\right) - \eta e V_{e,c},$$

$$\Delta U_n^c = \delta\left(n + \frac{1}{2}\right) + (1-\eta) e V_{e,c},$$

where $\delta = e^2/C$, $C = C_e + C_c$ is the net capacitance, and $C_{e(c)}$ is the emitter (collector) capacitance. In Eq. (A1), the electron Keldysh Green's function[20] $G^\pm$ in the well is defined in the $\{\mathbf{r},t\}$ presentation as

$$G^\pm(\mathbf{r},\mathbf{r}',t,t') = \pm i\langle \psi(\mathbf{r},t_\pm)\psi^\dagger(\mathbf{r}',t'_\mp)\rangle, \tag{A2}$$

where $\mathbf{r}$, $\mathbf{r}'$ are electron coordinates and $t_\pm$, $t'_\mp$ are the time moments assigned to points lying either on the positive (+) or on the negative (−) branch of the contour c circled around the time axis $-\infty < t < \infty$; $\langle\cdots\rangle$ means averaging[20] with full Hamiltonian $\hat{\mathcal{H}}$ which includes all the interactions in the system. Following Ref. 19 one may introduce the auxiliary right-moving ($\kappa=1$) free fermion Green's Keldysh function as

$$G_{10}^\pm = \frac{i\pi T/v_F}{\sinh[\pi T(x - v_F t)/v_F]} \pm i\pi\delta(x - v_F t), \tag{A3}$$

and for the left-moving ($\kappa=2$) free fermion $G_{20}^\pm = [G_{10}^\pm\{v_F \to -v_F\}]^*$. The Fourier transforms of Eq. (A3) at $x=0$ are

$$G_{10}^+(\varepsilon) = i\mathcal{N}(\varepsilon)[1 - \mathcal{G}_0(\varepsilon)],$$

$$G_{10}^-(\varepsilon) = -i\mathcal{N}(\varepsilon)\mathcal{G}_0(\varepsilon), \tag{A4}$$

where $\mathcal{N}(\varepsilon)$ is the single-electron density of states inside the well, and $\mathcal{G}_0(\varepsilon) = [1 - \tanh(\varepsilon/2T)]/2 = [\exp(\varepsilon/T) + 1]^{-1}$ is the equilibrium electron distribution function in the well. The electron tunneling rate $\Gamma_k^{e,c}$ is modified by the external ac bias as

$$\Gamma^{e,c}(t) \to \Gamma^{e,c}(t) e^{i\alpha_{e,c}\cos\Omega t} = \int d\varepsilon' \Gamma^{e,c}(\varepsilon') e^{i\varepsilon' t/\hbar} e^{i\alpha_{e,c}\cos\Omega t}.$$

The backward Fourier transform gives

$$\begin{aligned}\Gamma^{e,c}(\varepsilon) &= \int dt \int d\varepsilon' \Gamma^{e,c}(\varepsilon') e^{i\alpha\cos\Omega t} e^{-i\varepsilon t/\hbar + i\varepsilon' t/\hbar} \\ &= \sum_m J_m^2(\alpha_{e,c}) \int d\varepsilon' \int dt \Gamma^{e,c}(\varepsilon') e^{im\Omega t - i\varepsilon t/\hbar + i\varepsilon' t/\hbar} \\ &= \sum_m J_m^2(\alpha_{e,c}) \int d\varepsilon' \Gamma^{e,c}(\varepsilon') \delta(m\hbar\Omega - \varepsilon + \varepsilon'),\end{aligned} \tag{A5}$$

which indicates that photons of the external ac field shift energies of tunneling electrons by $m\hbar\Omega$. Then

$$\begin{aligned}w_+(m) - w_-(m) = \int d\varepsilon J_m^2(\alpha_{e,c}) \Gamma^{e,c}[\varepsilon_{k,e(c)}^m] (f[\varepsilon_{e(c)}^m] G_m^-(\varepsilon,\Omega) \\ + \{1 - f[\varepsilon_{e(c)}^m]\} G_m^+(\varepsilon,\Omega)).\end{aligned}$$

If the energy dependence of $\Gamma^{e,c}(\varepsilon_{k,e(c)}^m)$ is negligible, one gets

$$w_{+}^{e,c}(n,m) - w_{-}^{e,c}(n,m) = \Gamma^{e,c} J_m^2(\alpha_{e,c}) \int d\varepsilon \{ f_{+}^{e(c)} G^{-} + [1 - f_{-}^{e(c)}] G^{+} \}$$

$$= \Gamma^{e,c} J_m^2(\alpha_{e,c}) \int d\varepsilon \{ f_{+}^{e(c)} (\mathcal{K} + i \,\mathrm{Re}\, \mathcal{K}) + [1 - f_{-}^{e(c)}] (\mathcal{K} - i \,\mathrm{Re}\, \mathcal{K}) \}$$

$$= \Gamma^{e,c} J_m^2(\alpha_{e,c}) \int d\varepsilon \{ \mathcal{K} [1 + f_{+}^{e(c)} - f_{-}^{e(c)}] + i \,\mathrm{Re}\, \mathcal{K} [f_{+}^{e(c)} + f_{-}^{e(c)} - 1] \},$$

where we used the short notations $f(\varepsilon_{e(c)}^{m\pm}) \to f_{\pm}^{e(c)}$ and $G^{\pm} = \mathcal{K} \mp i \,\mathrm{Re}\, \mathcal{K}$. Here $\mathcal{K} = (G^{-} + G^{+})/2$ is the full electron correlator from which the retarded Green's function is obtained as $G^R(x,t) = -2i\theta(t) \mathrm{Re}\, \mathcal{K}(x,t)$. The time-averaged partial electric current I^e between the emitter and the quantum well takes the form

$$I^e = e \sum_n \zeta_n [w_{+}^{e}(n,m) - w_{-}^{e}(n,m)] = e\Gamma^e \int d\varepsilon \sum_{nm} J_m^2(\alpha_{e,c}) \zeta_n \{ \mathcal{K}(\varepsilon) + \mathcal{K}(\varepsilon) [f_{+}^{e(c)} - f_{-}^{e(c)}] + \mathrm{Im}\, \mathcal{K}(\varepsilon) [1 - f_{+}^{e(c)} - f_{-}^{e(c)}] \}$$

$$= e\Gamma^e \sum_n \zeta_n n + e\Gamma^e \int d\varepsilon \sum_{nm} J_m^2(\alpha_{e,c}) \zeta_n \mathcal{K}(\varepsilon) [f_{+}^{e(c)} - f_{-}^{e(c)}] + e\Gamma^e \int d\varepsilon \sum_{nm} J_m^2(\alpha_{e,c}) \zeta_n \,\mathrm{Im}\, \mathcal{K}(\varepsilon) [1 - f_{+}^{e(c)} - f_{-}^{e(c)}],$$

where the number of extra electrons in the well is $n = \Sigma_k \mathcal{K}(\varepsilon)/(2\pi i)$. The electron tunneling between the quantum well and the electrodes causes a time evolution of the probability ζ_n to find n electrons inside the well. The time dependence of $\zeta_n(t)$ satisfies the master equation[24]

$$\dot{\zeta}_n = w_{n+1}^{-} \zeta_{n+1} + w_{n-1}^{+} \zeta_{n-1} - (w_n^{+} + w_n^{-}) \zeta_n. \tag{A6}$$

The collector part of the electric current inside the well follows from the equilibrium condition

$$0 \equiv I^e - I^c = \frac{2}{h} \cdot e\Gamma^e \int d\varepsilon \sum_n \zeta_n [\mathcal{K}(\varepsilon) J_m^2(\alpha_e)(f_{+}^{e} - f_{-}^{e})$$

$$- \mathrm{Im}\, \mathcal{K}(\varepsilon) J_m^2(\alpha_e)(1 - f_{+}^{e} - f_{-}^{e})]$$

$$- e\Gamma^c \int d\varepsilon \sum_n \zeta_n [\mathrm{Im}\, \mathcal{K}(\varepsilon) J_m^2(\alpha_c)(1 - f_{+}^{c} - f_{-}^{c})$$

$$- \mathcal{K}(\varepsilon) J_m^2(\alpha_c)(f_{+}^{c} - f_{-}^{c})] - e(\Gamma^e + \Gamma^c) \sum_n \zeta_n n.$$

The above equation gives

$$e[\Gamma^e + \Gamma^c] \sum_n \zeta_n n = \frac{2}{h} \int d\varepsilon \sum_n \zeta_n [\mathcal{K}(\varepsilon)(e\Gamma^e J_m^2(\alpha_e)[f_{+}^{e} - f_{-}^{e}]$$

$$+ e\Gamma^c J_m^2(\alpha_c)[f_{+}^{c} - f_{-}^{c}])$$

$$- \mathrm{Im}\, \mathcal{K}(\varepsilon)(e\Gamma^e J_m^2(\alpha_e)[1 - f_{+}^{e} - f_{-}^{e}]$$

$$+ e\Gamma^c J_m^2(\alpha_c)[1 - f_{+}^{c} - f_{-}^{c}])].$$

The average number of electrons in the well is

$$\langle n \rangle = \sum_n \zeta_n n + n_{\mathrm{G}},$$

where $n = \Sigma_k \mathcal{K}(\varepsilon)/(2\pi i)$, $\mathcal{K} = (G^{-} + G^{+})/2$ is the full electron correlator, and $G^{\pm}$ is the electron Keldysh Green's function (A4). The second term n_{G} is controlled by the gate voltage $V_{\mathrm{G}} \neq 0$ applied to the quantum well as shown in Fig. 1. Then one gets the following expression for the average number of electrons in the well:

$$\langle n \rangle = \frac{2}{h} \frac{1}{\Gamma^e + \Gamma^c} \int d\varepsilon \sum_{nm} \zeta_n [\mathcal{K}(\varepsilon)(\Gamma^e J_m^2(\alpha_e)[f_{+}^{e} - f_{-}^{e}]$$

$$+ \Gamma^c J_m^2(\alpha_c)[f_{+}^{c} - f_{-}^{c}]) + \mathrm{Im}\, \mathcal{K}(\varepsilon)(\Gamma^e J_m^2(\alpha_e)[1 - f_{+}^{e} - f_{-}^{e}]$$

$$+ \Gamma^c J_m^2(\alpha_c)[1 - f_{+}^{c} - f_{-}^{c}])] + n_{\mathrm{G}}. \tag{A7}$$

Equation (A7) actually determines the chemical potential $\mu_{\mathcal{T}}(n)$ of electrons in the well. In absence of the SET one gets $f(\varepsilon_{+}^{e}) = f(\varepsilon_{-}^{e})$ and the first term under $\int d\varepsilon$ in Eq. (A7) vanishes. Then one simply gets

$$\frac{I^e + I^c}{2} = \frac{e\Gamma^e}{h} \int d\varepsilon \sum_n \zeta_n [\mathcal{K}(\varepsilon) J_m^2(\alpha_e)(f_{+}^{e} - f_{-}^{e})$$

$$- \mathrm{Im}\, \mathcal{K}(\varepsilon) J_m^2(\alpha_e)(1 - f_{+}^{e} - f_{-}^{e})]$$

$$+ e\Gamma^c \int d\varepsilon \sum_n \zeta_n [\mathrm{Im}\, \mathcal{K}(\varepsilon) J_m^2(\alpha_c)(1 - f_{+}^{c} - f_{-}^{c})$$

$$- \mathcal{K}(\varepsilon) J_m^2(\alpha_c)(f_{+}^{c} - f_{-}^{c})] - e(\Gamma^e - \Gamma^c) \sum_n \zeta_n n.$$

If one also sets $n_{\mathrm{G}} = 0$ (i.e., when no gate voltage is applied $V_{\mathrm{G}} \equiv 0$) then

$$\frac{I^e + I^c}{2} = \frac{e\Gamma^e}{h} \int d\varepsilon \sum_{k,n} \zeta_n [\mathcal{K}(\varepsilon) J_m^2(\alpha_e)(f_{+}^{e} - f_{-}^{e})$$

$$- \mathrm{Im}\, \mathcal{K}(\varepsilon) J_m^2(\alpha_e)(1 - f_{+}^{e} - f_{-}^{e})]$$

$$+ e\Gamma^c \sum_{k,n} \zeta_n [\mathrm{Im}\, \mathcal{K}(\varepsilon) J_m^2(\alpha_c)(1 - f_{+}^{c} - f_{-}^{c})$$

$$- \mathcal{K}(\varepsilon) J_m^2(\alpha_c)(f_{+}^{c} - f_{-}^{c})] - \frac{2e}{h} \frac{\Gamma^e - \Gamma^c}{\Gamma^e + \Gamma^c} \int d\varepsilon \sum_{nm} \zeta_n \{ \mathcal{K}(\varepsilon)$$

$$\times \Gamma^e J_m^2(\alpha_e)(f_+^e - f_-^e) + \Gamma^c J_m^2(\alpha_c)(f_+^c - f_-^c)]$$
$$- \mathrm{Im}\, \mathcal{K}(\varepsilon)[e\Gamma^e J_m^2(\alpha_e)(1 - f_+^e - f_-^e)$$
$$+ e\Gamma^c J_m^2(\alpha_c)(1 - f_+^c - f_-^c)]\}.$$

Using that

$$\Gamma_n = \Gamma^{e(c)}\left(1 \mp \frac{\Gamma^e - \Gamma^c}{\Gamma^e + \Gamma^c}\right) = \frac{2\Gamma^e\Gamma^c}{\Gamma^e + \Gamma^c}$$

the dc photon-assisted single-electron tunneling electric current across the quantum well reads

$$I = \frac{I^e + I^c}{2} = \Gamma_n \frac{2e}{h}\int d\varepsilon \sum_{nm} \zeta_n \{\mathcal{K}(\varepsilon)[J_m^2(\alpha_e)(f_+^e - f_-^e) - J_m^2(\alpha_c)$$
$$\times (f_+^c - f_-^c)] + \mathrm{Im}\, \mathcal{K}(\varepsilon)[J_m^2(\alpha_e)(f_+^e + f_-^e) - J_m^2(\alpha_c)(f_+^c + f_-^c)]\}. \quad \text{(A8)}$$

In equilibrium one makes use of the Fourier transform

$$\mathcal{K}_0(\mathbf{k}) = \frac{i}{2}\tanh\left(\frac{\beta v_F|\mathbf{k}|}{2}\right) = \frac{i}{2}[1 - 2\mathcal{G}_0(\beta v_F|\mathbf{k}|)],$$

where $\mathcal{G}_0(\varepsilon) = 1/[\exp(\varepsilon/T) + 1]$ and $\mathbf{k}$ is the fermion momentum. The noninteractive equilibrium right-moving fermion correlator $\mathcal{K}_0(0,t)$ is

$$\mathcal{K}_0(x,t) = \frac{i}{x - v_F t + i\delta}\frac{\pi(x - v_F t)/\beta v_F}{\sinh[\pi(x - v_F t)/\beta v_F]},$$

where $\delta \to +0$. The electron distribution function $\mathcal{G}_\varepsilon$ is introduced by the ansatz (see, e.g., Ref. 25)

$$\mathcal{K}(\varepsilon) = \mathrm{Im}\, \mathcal{K}(\varepsilon)(1 - 2\mathcal{G}_\varepsilon). \quad \text{(A9)}$$

This gives the expression for the net time-averaged electric current across the double-barrier junction as follows:

$$I = \Gamma_n \frac{2e}{h}\int d\varepsilon \sum_{nm} \zeta_n\, \mathrm{Im}\, \mathcal{K}(\varepsilon)\{J_m^2(\alpha_e)[f_+^e + \mathcal{G}_\varepsilon(f_-^e - f_+^e)]$$
$$- J_m^2(\alpha_c)[f_+^c + (f_-^c - f_+^c)\mathcal{G}_\varepsilon]\}. \quad \text{(A10)}$$

From Eq. (A10) in the limits $\alpha_{e,c} = 0$ one easily recovers the expressions for tunneling current used in the main text.

*http://kyiv.phys.northwestern.edu

[1] M. S. Dresselhaus, G. Dresselhaus, and P. Avouris, *Carbon Tubes: Synthesis, Structure, Properties, and Applications* (Springer, New York, 2001).

[2] E. S. Snow, F. K. Perkins, E. J. Houser, S. C. Badescu, and T. L. Reinecke, Science **307**, 1942 (2005).

[3] V. P. Wallace, A. J. Fitzgerald, S. Shankar, R. J. Pye, and D. D. Arnone, Br. J. Dermatol. **151**, 424 (2004).

[4] S. E. Shafranjuk, Phys. Rev. B **76**, 085317 (2007).

[5] J. Zhang, A. Boyd, A. Tselev, M. Paranjape, and P. Barbara, Appl. Phys. Lett. **88**, 123112 (2006); A. Tselev, K. Hatton, M. S. Fuhrer, M. Paranjape, and P. Barbara, Nanotechnology **15**, 1475 (2004).

[6] J. Zhang, A. Tselev, Y. Yang, K. Hatton, P. Barbara, and S. Shafraniuk, Phys. Rev. B **74**, 155414 (2006).

[7] D. Gunlycke, C. J. Lambert, S. W. D. Bailey, D. G. Pettifor, G. A. D. Briggs, and J. H. Jefferson, Europhys. Lett. **73**, 759 (2006).

[8] B. Babić and C. Schönenberger, Phys. Rev. B **70**, 195408 (2004).

[9] J. Cao, Q. Wang, and H. Dai, Nature Mater. **4**, 745 (2005).

[10] W. G. van der Wiel, S. De Franceschi, T. Fujisawa, J. M. Elzerman, S. Tarucha, and L. P. Kouwenhoven, Science **289**, 2105 (2000).

[11] J. W. Mintmire and C. T. White, Phys. Rev. Lett. **81**, 2506 (1998).

[12] C. Kane, L. Balents, and M. P. A. Fisher, Phys. Rev. Lett. **79**, 5086 (1997).

[13] S. Tomonaga, Prog. Theor. Phys. **5**, 544 (1950); J. M. Luttinger, J. Math. Phys. **4**, 1154 (1963).

[14] M. Bockrath, D. H. Cobden, J. Lu, A. G. Rinzler, R. E. Smalley, L. Balents, and P. L. McEuen, Nature (London) **397**, 598 (1999); Z. Yao, H. W. Ch. Postma, L. Balents, and C. Dekker, *ibid.* **402**, 273 (1999).

[15] H. Ishii, H. Kataura, H. Shiozawa, H. Yoshioka, H. Otsubo, Y. Takayama, T. Miyahara, S. Suzuki, Y. Achiba, M. Nakatake, T. Narimura, M. Higashiguchi, K. Shimada, H. Namatame, and M. Taniguchi, Nature (London) **426**, 540 (2003).

[16] P. Recher, N. Y. Kim, and Y. Yamamoto, Phys. Rev. B **74**, 235438 (2006).

[17] Yu. V. Nazarov and L. I. Glazman, Phys. Rev. Lett. **91**, 126804 (2003).

[18] R. Tarkiainen, M. Ahlskog, J. Penttila, L. Roschier, P. Hakonen, M. Paalanen, and E. Sonin, Phys. Rev. B **64**, 195412 (2001).

[19] V. See, in *Highly Conducting One-Dimensional Solids*, edited by J. Devreese *et al.* (Plenum, New York, 1979).

[20] L. V. Keldysh, Sov. Phys. JETP **20**, 1018 (1965).

[21] S. Datta, *Electronic Transport in Mesoscopic Systems* (Cambridge University Press, Cambridge, 1997).

[22] D. E. Feldman, S. Scheidl, and V. M. Vinokur, Phys. Rev. Lett. **94**, 186809 (2005).

[23] M. Trushin and A. L. Chudnovskiy, Europhys. Lett. **82**, 17008 (2008).

[24] D. V. Averin, A. N. Korotkov, and K. K. Likharev, Phys. Rev. B **44**, 6199 (1991).

[25] V. F. Elesin and Yu. V. Kopaev, Sov. Phys. Usp. **24**, 116 (1981).

[26] R. Egger and A. O. Gogolin, Phys. Rev. Lett. **79**, 5082 (1997).

[27] J. O'Keeffe, C. Wei, and K. Cho, Appl. Phys. Lett. **80**, 676 (2002).

[28] C.-W. Chen, M.-H. Lee, and S. J. Clark, Nanotechnology **15**, 1837 (2004).

[29] P.-W. Chiu, M. Kaempgen, and S. Roth, Phys. Rev. Lett. **92**, 246802 (2004).

[30] Y. Li, S. V. Rotkin, and U. Ravaioli, Nano Lett. **3**, 183 (2003).